IEEE Access
Multidisciplinary | Rapid Review | Open Access Journal

IEEE POWER & ENERGY SOCIETY SECTION

Received December 3, 2020, accepted December 24, 2020, date of publication December 30, 2020, date of current version January 8, 2021.

Digital Object Identifier 10.1109/ACCESS.2020.3048175

Cluster-Based Predictive PCC Voltage Control of Large-Scale Offshore Wind Farm

THAI-THANH NGUYEN[1], (Member, IEEE), AND HAK-MAN KIM[2], (Senior Member, IEEE)
[1]Department of Electrical and Computer Engineering, Clarkson University, Potsdam, NY 13699, USA
[2]Department of Electrical Engineering, Incheon National University, Incheon 406-772, South Korea

Corresponding author: Hak-Man Kim (hmkim@inu.ac.kr)

This work was supported by Korea Electric Power Corporation under Grant R18XA03.

ABSTRACT A large number of wind turbine generators in the large-scale offshore wind farm system poses a challenge to the wind farm control system due to the computational burden in the central control methods or the complexity of the communication network in the decentralized control strategies. A hybrid control method based on the distributed consensus control and the central model predictive control is proposed in this study to overcome the problem. Typically, the wind turbine generators in the large-scale offshore wind farm system are clustered into several groups. The consensus-based distributed reactive power coordination control is proposed to each cluster and the centralized predictive voltage control is used to manage the total reactive powers of all clusters and regulate the voltage at the point of common coupling. The gradient-descent algorithm for the optimal design of the consensus-based cluster control is presented firstly. Based on the convergence property of the consensus control, the equivalent model of the total reactive power response of each cluster is identified, which is used for the design of the centralized predictive voltage control. Eigenvalue analysis of the proposed predictive control strategy is carried out to verify the stability of the distributed and predictive control systems. The robustness of the proposed predictive controller is evaluated in the conditions of significant model errors due to the communication delay in each cluster. A comparison study with the full distributed control based on consensus algorithm is presented to demonstrate the effectiveness of the proposed control method. The feasibility of the proposed predictive controller is evaluated by the control-hardware-in-the-loop simulation using OPAL-RT Technologies. An additional comparison study in term of computation time with the central control method is also carried out. Real-time simulation results show the superior performance of the proposed hybrid method compared to the full distributed consensus controller or the central control strategies.

INDEX TERMS Distributed control, reactive power control, consensus algorithm, wind farm control, predictive voltage control, model predictive control.

I. INTRODUCTION

The offshore wind energy has been becoming prominent due to the restriction of the land availability for onshore installation [1], [2]. Since the strength and uniformity of wind over the ocean are much stronger than over land, the offshore wind farms have the potential to produce impressive wind power with high efficiency as compared to the traditional wind farms. The development of large-scale offshore wind farms has attracted more attention recently. The fast-growing penetration of offshore wind farms poses a challenge to the voltage stability of the power systems [3]. Voltage stability refers to the ability to maintain steady voltages at all buses in a power system after being subjected to a disturbance. When the penetration of offshore wind farms significantly increases, large voltage drops may occur suddenly, which has a significant impact on the balance of real and reactive powers in power system. Large oscillation of real and reactive powers may force the voltage to vary beyond the boundary of stability. Thus, maintaining voltage stability in case of large-scale offshore wind farm is challenging.The operation of offshore wind farms is required to have the capability of voltage support at the point of common coupling (PCC).

Wind turbine generators (WTGs) are commonly coupled with the power converters to maximally capture wind powers. Thus, each WTG could supply real and reactive

The associate editor coordinating the review of this manuscript and approving it for publication was Guangya Yang.

powers independently due to the controllers of power converters. Coordinating reactive power generations among WTGs could improve the voltage stability of the power system [4]. Various control strategies have been presented for reactive power coordination and PCC voltage control in wind farms, which could be categorized into two strategies: centralized and decentralized. In the centralized control strategies, a central controller supervises the reactive power injected to the grid and controls the PCC voltage. The central controller gathers all global information to decide the optimal set point for each WTG. The centralized control strategies could be based on the proportional-integral (PI) regulators [5]–[7] or optimization algorithms such as integer optimization [8].

The model predictive control (MPC) of the wind farm system has been received more attention due to its advantages of robustness and easy inclusion of variable constraints. The principle of receding the control horizon makes the MPC techniques be suitable for real-time optimization control since only the finite-horizon control problem is solved. The MPC-based coordinated control among WTGs and static Var compensator has been presented in [9]. In case the offshore wind farm connects to the utility grid through the high voltage direct current (HVDC) system, an MPC coordination control between WTGs and power converters of the HVDC system was presented in [10]. In [11], the presented MPC strategy involved both active and reactive powers to compensate for the voltage variations. An important factor of the MPC strategy for the real-time control problem is its computation time, in which the execution of the MPC algorithm has to be fast enough to ensure that the optimal control signals are completely found over a fixed time interval. Thus, the problem of the computational burden of the central MPC strategy in the case of a large-scale wind farm system should be addressed. The decentralized MPC strategy for coordinated voltage control was presented in [12], in which the central MPC with an unconstrained optimization problem is solved firstly, then the local controller solves the constraint-optimization problem. The computational burden in the central MPC is reduced by solving the optimization problem without any constraints [12].

The decentralized strategies have been presented to overcome the problem of computation burden in centralized strategies. In the decentralized approaches, the optimal solution could be found by using some partial information. In [13], three strategies for PCC voltage regulation were discussed and an improved distributed voltage control was presented. The consensus-based distributed voltage controls of the large-scale wind farm were presented in [14]. The distributed cooperation was applied for coordination among sub-wind farm clusters whereas a central controller was used to manage the reactive powers of WTGs in each cluster. The decentralized MPC strategies for the wind farm system have been presented in [15], [16], in which the communication network is utilized to share information among the distributed MPC controller. Since the distributed generations (DGs) in the microgrid (MG) system could be considered as WTGs, the developed strategies for MG system would be able to apply for wind farms. Distributed control strategies for accurate reactive power sharing among DGs were presented in [17]–[21]. Voltage control layer could be added in addition to the reactive power control to restore the system voltage [22]–[24]. However, these solutions face the problem of communication burden in the large-scale system since the number of agents significantly increases. The control algorithm in the decentralized method could be optimally designed to overcome the problem of complex communication network [25], [26]. These solutions are attractive since they can reduce the complexity of communication network whereas the control performance is retained.

Existing centralized and decentralized strategies should be further improved to be applicable for the large-scale offshore wind farm. Although the centralized MPC strategies offer the benefits of robustness and fast control responses, the performance of these MPC strategies in case of large-scale system could be significantly affected by the limitation of computation. Decentralized strategies would be more attractive since they can improve the control reliability compared to the centralized methods. However, the complexity of the communication network could retrain their applications on the large-scale system. To overcome the problems of both centralized and decentralized control methods, this study proposes a hybrid control method for the large-scale wind farm system, which consists of the consensus-based distributed control of each cluster and the centralized predictive voltage control of the wind farm system. The proposed strategy has the advantages of both centralized and decentralized methods such as high robustness and high reliability. Since the centralized predictive voltage controller only supervises the clustering wind turbines, the computational burden would be significantly reduced. In addition, the consensus-based distributed control in each cluster could enhance the reliability of the control system. Since the number of WTGs in each cluster could be chosen for an optimal communication network, the complexity and convergence time of the consensus-based distributed control could be significantly reduced. The main contributions of this study are listed as follows,

- A gradient-descent algorithm for the optimal design of the consensus-based distributed cluster control is proposed, which can reduce the complexity of the communication network.
- A hybrid control method based on distributed consensus control and centralized predictive voltage control is proposed to coordinate reactive power generations and regulate the PCC voltage of the offshore wind farm system.
- The control-hardware-in-the-loop simulation platform is developed to verify the proposed hybrid control strategy of offshore wind farm system.

The rest of this paper is organized as follows. Section II presents the proposed cluster-based wind farm control method. The design of the consensus-based cluster control and the centralized predictive voltage control are described in

this section. The real-time simulation results and eigenvalue analysis are provided in Section III, including the evaluation of the proposed predictive controller under the conditions of significant model errors. Section IV summarizes the main finding of this study.

II. CLUSTER-BASED WIND FARM CONTROL METHODOLOGY

A typical clustering offshore wind farm system is shown in Fig. 1, in which each cluster is composed of group WTGs connected in series. The wind farm control strategy is divided into three control layers such as local control layer (LC), cluster control layer (CC), and centralized predictive PCC voltage control layer (C_{MPC}), as shown in Fig. 2. The central model predictive controller is applied for the wind farm control level. It managers the total reactive power of offshore wind farm and generate the reactive power reference for each cluster in wind farm. The distributed consensus control layer is applied for the cluster control layer, which receives the reactive power reference from the central controller and generates the reactive power reference to each wind turbine in such cluster. The local control layer, which only uses the local information of WTG, is in charge of regulating output active and reactive powers of each WTG. The reactive power reference (Q_i^*) for the local control layer is received from the cluster control layer that is responsible for the distributed coordination control of each cluster. The cluster control layer employs the consensus algorithm to achieve reactive power coordination among WTGs in each cluster. The total reactive power required for each cluster is provided by a central voltage control layer, which is based on the model predictive control (MPC) technique. The central MPC layer gathers all information on reactive power generated by each cluster. The control signal to each cluster (Q_{ci}^*) is calculated by the central MPC based on the reactive power and PCC voltage (v_{pcc}) information. The control sequence of the three control layers is shown in Fig. 3, in which three layers are executed with different sampling times. The local control layer is the fastest control layer, which ensures the stability of the converter controller whereas the central MPC layer is the slowest control layer to regulate the PCC voltage. The coupling effect of three control layers on the system stability is reduced by properly designing these sampling times. Besides, the sampling time has to be longer than the computation time of each control layer to ensure that the control signals are completely found.

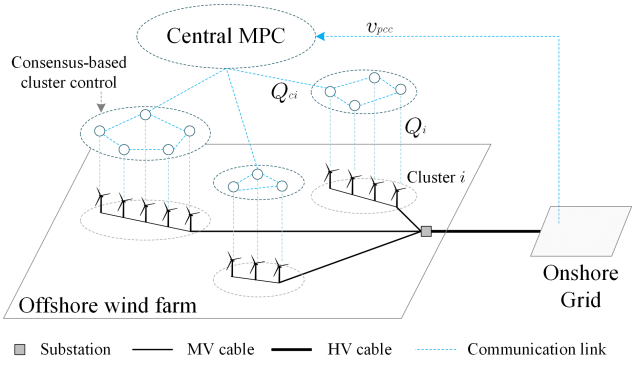

FIGURE 1. Cluster-based hybrid wind farm control strategy.

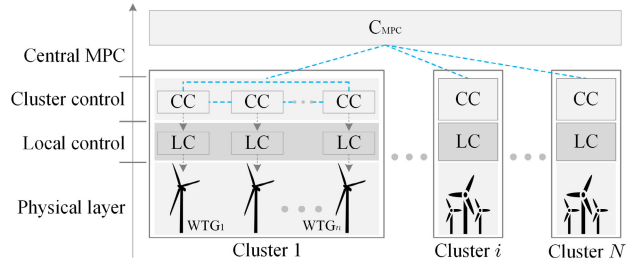

FIGURE 2. Hierarchical control of offshore wind farm system with three control layers.

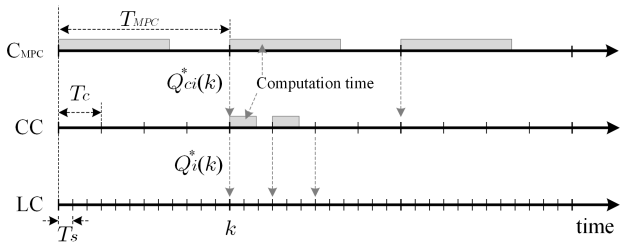

FIGURE 3. Control sequence of three layers with different sampling times.

A. CONSENSUS-BASED CLUSTER CONTROL

The configuration of the type-4 WTG is shown in Fig. 4, which consists of a permanent magnet synchronous generator and a back-to-back (BTB) converter. The BTB converter is used to regulate the output WTG powers, in which the machine side converter (MSC) is in charge of the generator speed or torque control whereas the grid side converter(GSC) is responsible for the DC-link voltage and output reactive power regulation. Both converters are controlled by the rotating *dq*-reference frame with the proportional-integral regulators.

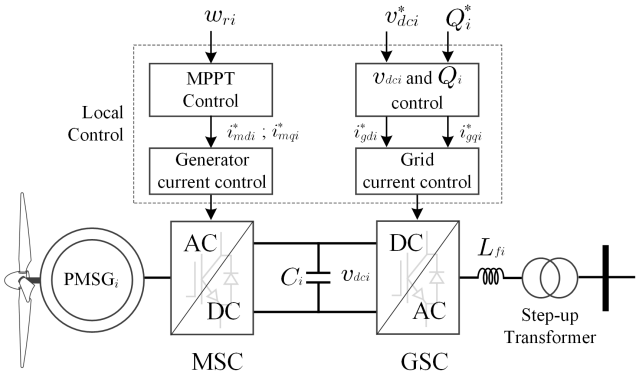

FIGURE 4. Local control of wind turbine generator, in which the reactive power reference (Q_i^*) is received form the cluster control layer.

In the proposed voltage control strategy, each WTG receives the reactive power reference (Q_i^*) from the cluster control layer. The communication network is utilized in the cluster control layer to realize the neighbor-to-neighbor information exchange, which is described by the graph-theoretic notation in this study. Each WTG$_i$ sends its reactive output power information (Q_i) to the neighbors and receives reactive information from the neighbors of WTG$_i$.

The communication link among WTGs is represented by an undirected graph $\mathbb{G} = (V, E)$ with the set of nodes $V = \{1, 2, \ldots, n\}$ and edges $E \in V^2$, in which n nodes represents the number of WTG controller and the set of edges E represents the communication links among these controllers. For example, the edge $E\{i, j\}$ indicates that the note $V\{i\}$ can receive information from node $V\{j\}$. The adjacency matrix that is associated with the graph G is $A = \{a_{ij}\}_{i,j=1,\cdots,n} \in \mathbb{R}^{n\times n}$, as given by (1).

$$a_{ij} = \begin{cases} 1 & \text{if } (i,j) \in E \\ 0 & \text{if } (i,j) \notin E \text{ or } i = j \end{cases} \tag{1}$$

The graph Laplacian matrix is represented by $L = \{l_{ij}\}_{i,j=1,\cdots,n} \in \mathbb{R}^{n\times n}$, with

$$l_{ij} = \begin{cases} \sum_{j=1, j\neq i}^{n} a_{ij} & \text{for } i = j \\ -a_{ij} & \text{for } i \neq j \end{cases} \tag{2}$$

In case the power ratings of wind turbine generators in each cluster are different, the reactive power generation of each wind turbine should be proportional to its power rating. Equation (3) shows the condition for accurate reactive power sharing among wind turbine generators in each cluster.

$$n_{qi}Q_i = n_{qj}Q_j \quad \forall i, j \in [1, n] \tag{3}$$

where n_{qi} and n_{qj} are the constant weights that are proportional to the power ratings of wind turbines i and j, respectively. The constant weight is given by

$$n_{qi} = S_{max}/S_i \tag{4}$$

where S_i is the power rating of wind turbine generator i and S_{max} is the maximum power rating in cluster.

The leader-following consensus algorithm with the control law of WTG$_i$ at time instant $k+1$ is proposed by (5). The consensus objective is to ensure the accurate reactive power sharing among wind turbine generators in each cluster.

$$Q_i(k+1) = n_{qi}Q_i(k) + \alpha \sum_{j\in V_i} \left(n_{qj}Q_j(k) - n_{qi}Q_i(k)\right) + b_i\left(\frac{1}{n}Q_{ci}^*(k) - n_{qi}Q_i(k)\right) \tag{5}$$

where Q_{ci}^* is the command from the central MPC layer; n is the number of the WTGs in each cluster; b_i equals 1 if the WTG$_i$ is the neighborhood of the leader and equals 0 otherwise; α is a constant edge-weight coefficient.

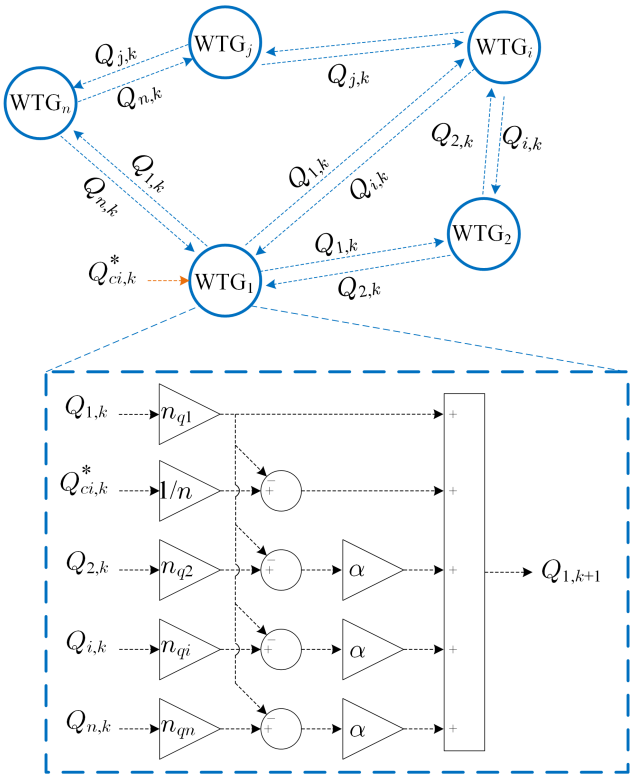

FIGURE 5. Diagram of the consensus-based cluster controller.

Fig. 5 shows the diagram of the consensus-based cluster controller, in which the WTG$_1$ is the leader and it communicates with WTG$_2$, WTG$_i$, and WTG$_n$. The reactive powers, which are received from the neighbors of WTG$_1$, are used to calculate the reactive power reference for the local control of WTG$_1$, as shown in this diagram.

The leader-following consensus algorithm is represented in the vector form, as given by (6).

$$Q(k+1) = WQ(k) + B_L\left(\frac{1}{n}Q_{ci}^*(k) - Q(k)\right) \tag{6}$$

where $W = I - \alpha L$; I is the identity matrix with size of n; $Q(k) = [n_{q1}Q_1(k), n_{q2}Q_2(k), \cdots, n_{qn}Q_n(k)]^\top$; $B_L = \text{diag}(b_1, b_2, \cdots, b_n)$.

The command signal (Q_{ci}^*) could be considered as a constant, thus, the control law given by (6) is rewritten as in (7).

$$\mathbf{u}(k+1) = W_c\mathbf{u}(k) \tag{7}$$

where

$$W_c = \begin{bmatrix} (1/n)I_{n\times n} & \mathbf{0}_{n\times n} \\ B_L & W - B_L \end{bmatrix}$$
$$\mathbf{u}(k) = [Q_{ci}^*(k), Q(k)]^\top \tag{8}$$

The proposed leader-following consensus algorithm for constant weight matrix W_c converges if the limit $\lim_{k\to\infty}\mathbf{u}(k)$ exists for $\forall\mathbf{u}(0) < \infty$, i.e,

$$\lim_{k\to\infty}\mathbf{u}(k) = \lim_{k\to\infty}W_c^k\mathbf{u}(0) = \mathbf{u}^* \tag{9}$$

where $\mathbf{u}^*$ is the limit of vector $\mathbf{u}$ when k approaches infinity.

Therefore, the convergence of the leader-following consensus algorithm depends only on the properties of the weight matrix W_c. Eigendecomposition of the matrix W_c is given by (10).

$$W_c = \mathbf{U}\Lambda\mathbf{U}^{-1} \tag{10}$$

where $\mathbf{U}$ is a square matrix of eigenvectors and $\Lambda = \text{diag}(\lambda_1, \lambda_2, \cdots, \lambda_n)$ is a diagonal matrix of eigenvalues.

The power of matrix W_c with eigendecomposition is given by (11).

$$W_c^k = \mathbf{U}\Lambda^k\mathbf{U}^{-1} \tag{11}$$

It can be seen that the convergence property of W_c^k depends on the eigenvalues Λ. The convergence is guaranteed if the absolute value of the biggest eigenvalue is equal to one, so that the $\lim_{k\to\infty}\Lambda^k$ exists. The convergence property of the leader-following consensus algorithm is ensured by properly designing the weight coefficients α. The convergence time of the consensus algorithm depends on the second largest eigenvalue of W_c, as given by (13).

$$\lambda_2 = \rho\left(W_c - \frac{1}{n}\mathbf{1}\mathbf{1}^\top\right) \tag{12}$$

$$\tau = \frac{1}{\log(1/\lambda_2)} \tag{13}$$

where $\mathbf{1}$ denotes the column vector with all ones; n is the number of WTGs in each cluster; and $\rho(\cdot)$ is the spectral radius.

The gradient descent (GD) algorithm is proposed in this study to find the optimal value of weight coefficient α that minimizes the second largest eigenvalue λ_2, resulting in the fast convergence speed, as given by Algorithm 1. The first step of GD algorithm is to initialize the constant edge-weight coefficient α_0 and learning rate λ. Based on this initialization, the second largest eigenvalue of matrix W_c is calculated. The partial derivative of second largest eigenvalue with respect to the constant edge-weight coefficient is found. Consequently, the value of constant edge-weight coefficient is updated based on the partial derivative. These steps are repeated until the change in the value of second largest eigenvalue is smaller than tolerance ϵ, and the optimal value of constant edge-weight is found.

To ensure the convergence condition of the consensus control system throughout the optimizing process, the value of the second largest eigenvalue λ_2 is set to infinity if the spectral radius of W_c is larger than one. The goal of the optimization process is to find the optimal value of α that not only optimizes the value of the second largest eigenvalue but also ensures that the largest absolute value of eigenvalues of W_c is equal or smaller than one.

B. CENTRALIZED PREDICTIVE PCC VOLTAGE CONTROL

The cluster control layer receives the command of reactive power from the central controller then it is equally divided to all WTGs in such cluster by the leader-following consensus algorithm. The convergence time of each cluster is optimally designed by the Algorithm 1. Table. 1 shows the optimal weight constant α of leader-following consensus controls of two clusters with the ring communication topology. Fig. 6 shows the eigenvalues two cluster controllers with 5 and 10 WTGs, respectively. It can be seen that the design of the consensus control guarantees the convergence property since all eigenvalues are located inside the unit circle. The dynamic response in time-domain of two clusters is shown in Figs. 7.

Algorithm 1 Optimizing α Based on the Gradient-Descent Algorithm

1: $i \leftarrow 0$, initialize α_0 and γ;
2: **repeat**
3: Calculate λ_2 based on α_i: $\lambda_2(i) \leftarrow \lambda_2|\alpha_i$;
4: $g_{\alpha i} \leftarrow \big(\lambda_2(i) - \lambda_2(i-1)\big)/\big(\alpha_i - \alpha_{i-1}\big)$;
5: $\alpha_{i+1} \leftarrow \alpha_i + \gamma g_{\alpha i}$;
6: $i \leftarrow i + 1$
7: **until** $\max|\lambda_2(i+1) - \min_i(\lambda_2(i))| < \epsilon$
8: **return** α_i;

TABLE 1. Optimal results using Algorithm 1.

Cluster	number of WTGs	optimal α	λ_2	τ_i
1	5	0.29	0.920	12.70 s
2	10	0.28	0.978	44.35 s

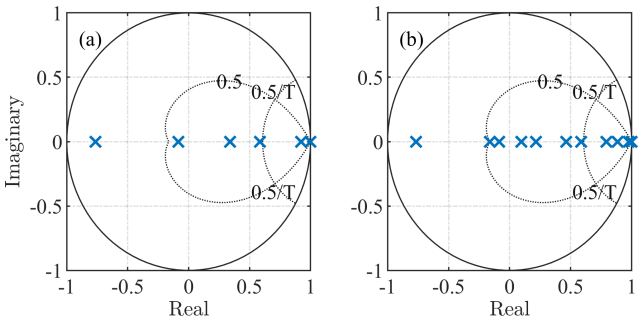

FIGURE 6. Eigenvalues of consensus-based cluster control: (a) cluster with 5 WTGs; (b) cluster with 10 WTGs.

It could be observed that the response of total reactive power generation in each cluster is similar to the first-order system with the time constant τ_{ci}, as given by (14).

$$Q_{ci} = \frac{1}{s\tau_{ci} + 1}Q_{ci}^* \tag{14}$$

The time-domain representation of (14) is given by (15).

$$Q_{ci}(t) = (1 - e^{t/\tau_{ci}})Q_{ci}^*(t) \tag{15}$$

Since the convergence time of the consensus-based cluster controller is known by (13), the time constant τ_{ci} can be determined by the convergence time of each cluster τ_i. It could be defined that the convergence time τ_i is equal to the time at which the output reactive power reaches to the values of 99% of reactive power reference, as in (16), then the time constant

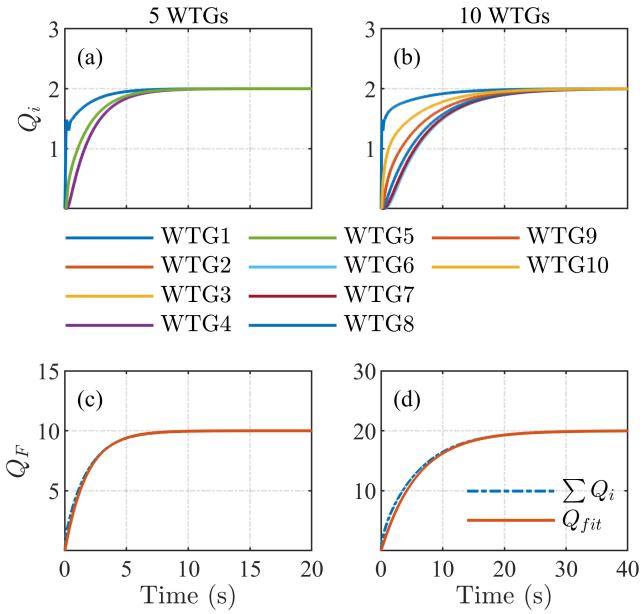

FIGURE 7. Tested offshore wind farm system: (a) and (b) show the output reactive powers of all WTGs in two clusters; (c) and (d) show the total reactive power output of two clusters ($\sum Q_i$) and the equivalent first-order system responses of two clusters (Q_{ci}).

of each cluster τ_{ci} is given by (17). Total output reactive powers of two clusters and their first-order approximation responses are shown in Figs. 7(c) and (d), which indicates that the estimation of the first-order system is accurate for the design of the centralized predictive PCC voltage control.

$$0.99 \times Q_{ci}^*(t) = (1 - e^{\tau_i/\tau_{ci}})Q_{ci}^*(t) \tag{16}$$

$$\Rightarrow \tau_{ci} = -\tau_i / \ln(0.01) \tag{17}$$

Based on the value of time constant τ_{ci}, the dynamic model of each cluster is given by (18).

$$\dot{Q}_{ci} = -\frac{1}{\tau_{ci}} Q_{ci} + \frac{1}{\tau_{ci}} Q_{ci}^* \tag{18}$$

Fig. 8 shows the simplified offshore wind farm system connected to the equivalent source, which is used for the analysis of the PCC voltage control. Total active and reactive powers delivering to the utility grid are given by (19) and (20).

$$P_W = \frac{v_{grid}}{R_e^2 + X_e^2} \left[R_e (v_{pcc} \cos\delta - v_{grid}) + X_e v_{pcc} \sin\delta \right] \tag{19}$$

$$Q_W = \frac{v_{grid}}{R_e^2 + X_e^2} \left[-R_e v_{pcc} \sin\delta + X_e (v_{pcc} \cos\delta - v_{grid}) \right] \tag{20}$$

where P_W and Q_W are the real and reactive powers injected to the utility grid; R_e and X_e are the resistance and

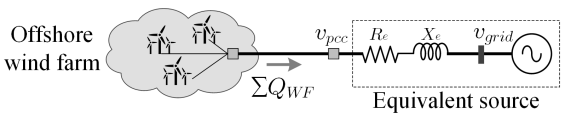

FIGURE 8. Offshore wind farm connected to the equivalent source.

inductance of transmission network; δ is the phase-angle difference between two voltages.

Since the resistance of the transmission network is typically much smaller than the inductance, the resistance could be neglected when calculating active and reactive powers. In addition, because the phase-angle difference δ in such line is small, it could be assumed that $\sin\delta \approx \delta$ and $\cos\delta \approx 1$. Thus, the transferred powers in (19) and (20) could be rewritten as:

$$P_W \approx \frac{v_{grid}}{X_e} v_{pcc} \delta \tag{21}$$

$$Q_W \approx \frac{v_{grid}}{X_e} (v_{pcc} - v_{grid}) \tag{22}$$

$$\Rightarrow v_{pcc} \approx v_{grid} + \frac{Q_W X_e}{v_{grid}} \tag{23}$$

It could be seen in (23) that the variation of PCC voltage is mainly depended on the total injected reactive power of offshore wind farm and the inductance of transmission network. The grid voltage v_{grid} could be assumed to be constant due to strong grid, thus, the variation of PCC voltage can be given by (24).

$$\Delta v_{pcc} = \frac{X_e}{v_{grid}} \Delta Q_W \tag{24}$$

The variation of PCC voltage could be further simplified as in (25), in which the change in reactive power of offshore wind farm is equal to total reactive power of all clusters.

$$\Delta Q_W = \sum_{i=1}^{N} Q_{ci}$$

$$\Delta v_{pcc} = \frac{X_e}{v_{grid}} \sum_{i=1}^{N} Q_{ci} \tag{25}$$

where N is the number of clusters in the wind farm system; X_e is the equivalent inductance of the utility grid; v_{grid} is the grid voltage.

The objective of of central MPC is to minimize the variation of PCC voltage. The wind farm model in Fig. 9 is developed for the design of the central MPC, which includes the dynamic model of each cluster in (14) and the dynamic network model in (25). The input signal of cluster model is the reactive power reference from the central controller and the output of cluster model is the reactive power response. Total reactive powers of all clusters in offshore wind farm is considered as the input of dynamic network model and the variation of PCC voltage (Δv_{pcc}) is the output of wind farm model. The central MPC receives the information of PCC voltage variation from the wind farm model. The optimal reactive power set-point for each cluster (Q_{ci}^*) that minimizes the variation of PCC voltage is calculated by the central MPC.The open loop continuous-time state space model of wind farm system is given by (26).

$$\dot{Q} = A_c Q + B_c U \tag{26a}$$

$$\Delta v = C_c Q \tag{26b}$$

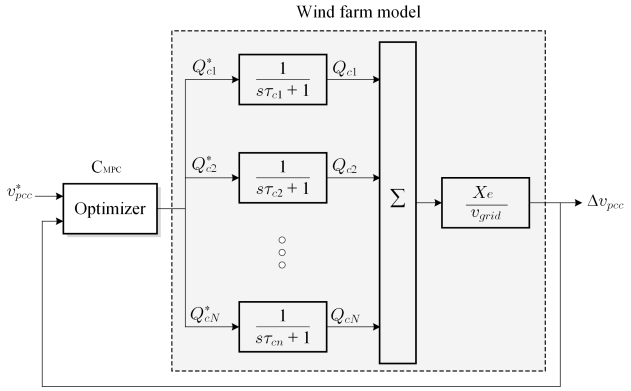

FIGURE 9. Dynamic model of offshore wind farm system.

where

$$A_c = \begin{bmatrix} -1/\tau_{c1} & 0 & \cdots & 0 \\ 0 & -1/\tau_{c2} & \cdots & 0 \\ \vdots & \vdots & \ddots & \vdots \\ 0 & 0 & \cdots & -1/\tau_{cN} \end{bmatrix} \quad (27)$$

$$B_c = \begin{bmatrix} 1/\tau_{c1} & 0 & \cdots & 0 \\ 0 & 1/\tau_{c2} & \cdots & 0 \\ \vdots & \vdots & \ddots & \vdots \\ 0 & 0 & \cdots & 1/\tau_{cN} \end{bmatrix} \quad (28)$$

$$\begin{aligned} C_c &= \frac{X_e}{v_{grid}} \begin{bmatrix} 1 & 1 & \cdots & 1 \end{bmatrix}_{1\times N} \\ Q &= [Q_{c1}, Q_{c2}, \cdots, Q_{cN}]^\top; \\ U &= [Q^*_{c1}, Q^*_{c2}, \cdots, Q^*_{cN}]^\top; \\ \Delta v &= \Delta v_{pcc}; \end{aligned} \quad (29)$$

The continuous state-space model in (26) is discretized with the sampling time of T_{MPC}, we obtains the discrete state-space model for the design of the central voltage controller, as given by (30).

$$Q(k+1) = A_d Q(k) + B_d U(k) \quad (30a)$$
$$\Delta v(k) = C_d Q(k) \quad (30b)$$

The objective of the proposed controller is to find the optimal future control actions (ΔU_d) to minimize the derivation of PCC voltage (Δv_{pcc}). Since the large-scale offshore wind farm system could consist of various types of WTGs with different capacities, a new matrix B_e defined in (31) is introduced to maintain accurate power sharing among WTGs in the wind farm system.

$$B_e = (1/S_w)\begin{bmatrix} S_{c1} & S_{c2} & \cdots & S_{cN} \end{bmatrix}^\top \quad (31)$$

where S_w is the capacity of offshore wind farm; S_{ci} with $\forall i \in [1, N]$ is the capacity of each cluster.

The discrete state-space model (30) is represented by (32).

$$Q(k+1) = A_d Q(k) + B_{de} U(k) \quad (32a)$$
$$\Delta v(k) = C_d Q(k) \quad (32b)$$

where $B_{de} = B_d B_e$.

Taking the difference operation of (32a), we have

$$\Delta Q(k+1) = A_d \Delta Q(k) + B_{de} \Delta U(k) \quad (33)$$

where

$$\begin{aligned} \Delta Q(k+1) &= Q(k+1) - Q(k) \\ \Delta Q(k) &= Q(k) - Q(k-1) \\ \Delta U(k) &= U(k) - U(k-1) \end{aligned}$$

In order to consider the dynamic of PCC voltage as a controlled variable, a new state vector in (34) is introduced.

$$x(k) = [\Delta Q(k)^\top, \Delta v(k)]^\top \quad (34)$$

The variation of PCC voltage at time instant $k+1$ is given by (35).

$$\begin{aligned} \Delta v(k+1) - \Delta v(k) &= C_d\big(Q(k+1) - Q(k)\big) \\ &= C_d \Delta Q(k+1) \\ &= C_d A_d \Delta Q(k) + C_d B_{de} \Delta U(k) \end{aligned} \quad (35)$$

The new state-space model involving the PCC voltage variable is given by (36).

$$x(k+1) = \mathbf{A}x(k) + \mathbf{B}\Delta U(k) \quad (36a)$$
$$\Delta v(k) = \mathbf{C}x(k) \quad (36b)$$

where

$$\begin{aligned} x(k) &= \begin{bmatrix} \Delta Q(k) \\ \Delta v(k) \end{bmatrix}; \quad \mathbf{A} = \begin{bmatrix} A_d & o_d^\top \\ C_d A_d & 1 \end{bmatrix}; \ \mathbf{B} = \begin{bmatrix} B_{de} \\ C_d B_{de} \end{bmatrix}; \\ \mathbf{C} &= \begin{bmatrix} o_d & 1 \end{bmatrix}; \quad o_d = \begin{bmatrix} 0 & 0 & \cdots & 0 \end{bmatrix}^\top \end{aligned}$$

The objective function of the central controller (J), which is used to find the reactive power set-point to each cluster (ΔU) that minimizes the PCC voltage deviation (Δv), is defined as follows

$$J(k) = (R_s - \Delta v)^\top Q(R_s - \Delta v) + \Delta U^\top R \Delta U \quad (37)$$

$$\begin{aligned} \text{s.t.: } & U_{min}(k+i|k) \le U(k+i|k) \le U_{max}(k+i|k) \\ & \forall i \in [0, N_c - 1] \end{aligned} \quad (38)$$

$$\begin{aligned} & x_{min}(k+i|k) \le x(k+i|k) \le x_{max}(k+i|k) \\ & \forall i \in [0, N_p] \end{aligned} \quad (39)$$

where Q and R are the weight matrices on the state variables and input variables, respectively; N_c is the control horizon; N_p is the prediction horizon;

$$\Delta v = \begin{bmatrix} \Delta v(k+1|k) \\ \Delta v(k+2|k) \\ \vdots \\ \Delta v(k+N_p|k) \end{bmatrix} = Fx(k|k) + \Phi \Delta U;$$

$$F = \begin{bmatrix} \mathbf{CA} & \mathbf{CA}^2 & \cdots & \mathbf{CA}^{N_p} \end{bmatrix}^\top;$$

$$\Phi = \begin{bmatrix} \mathbf{CB} & 0 & \cdots & 0 \\ \mathbf{CAB} & \mathbf{CB} & \cdots & 0 \\ \vdots & \vdots & \ddots & \vdots \\ \mathbf{CA}^{N_p-1}\mathbf{B} & \mathbf{CA}^{N_p-2}\mathbf{B} & \cdots & \mathbf{CA}^{N_p-N_c}\mathbf{B} \end{bmatrix};$$

$$x(k|k) = \begin{bmatrix} x(k+1|k) \\ x(k+2|k) \\ \vdots \\ x(k+N_p|k) \end{bmatrix}; \Delta U = \begin{bmatrix} \Delta U(k) \\ \Delta U(k+1) \\ \vdots \\ \Delta U(k+N_c-1) \end{bmatrix};$$
$$R_s = \Delta v^*(k) \begin{bmatrix} 1 & 1 & \cdots & 1 \end{bmatrix}^\top_{1\times N_p};$$

The objective of the central voltage control is to find the optimal control sequences ΔU that minimize the cost function (37). The quadratic programming is used to solve the objective function which is subjected to constraints (38) and (39). Since the optimal control sequences are found, only the first element of the control sequences $\Delta U(k|k)$ is applied for the cluster control layers.

The closed-loop state-space model of the wind farm system under the central controller is given by (40).

$$\mathbf{A}_{cl} = \mathbf{A} - \mathbf{B}K_m \tag{40}$$

where K_m is the state feedback gain matrix that is given by the first row of $(\Phi^\top\Phi + R)^{-1})\Phi^\top F$.

Thus, the closed-loop eigenvalues of the offshore wind farm with centralized predictive voltage control can be evaluated by the characteristic equation (41).

$$\det(\lambda I - \mathbf{A}_{cl}) = 0 \tag{41}$$

III. SIMULATION RESULTS

The proposed control strategy is evaluated in the offshore wind farm system with 30 WTGs dividing into three clusters. Table 2 shows the simulation parameters of the proposed control method and Fig. 10 shows the detailed configuration of the tested offshore wind farm system with total capacity of 145 MW. The parameters of the tested wind farm system is shown in Table 3. The feasibility of the proposed predictive control strategy of the offshore wind farm system is verified in the real-time simulation using OPAL-RT Technologies. Fig. 11 shows the setup of the real-time simulation, which

TABLE 2. Control parameters.

Sampling time	Time	Predictive control	Parameters
T_s	100 μs	N_p	10
T_c	0.1 s	N_c	5
T_{MPC}	0.5 s	weight gains of Q/R	1/0.003

TABLE 3. System parameters.

Parameter	Value
22.9 kV Cable	R = 0.103 Ω/km; L = 0.075 mH/km
Step-up transformer	6.6 kV / 22.9 kV
BTB converter	DC link voltage: 12 kV DC link capacitance: 2000 μ F Output inductance filter 0.5 H
Wind generator rating	3 MW; 5 MW; 10 MW
System frequency	60 Hz

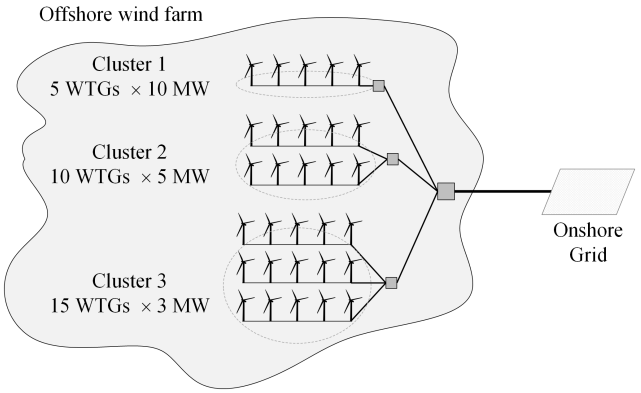

FIGURE 10. Tested offshore wind farm system with 30 WTGs grouped into three clusters.

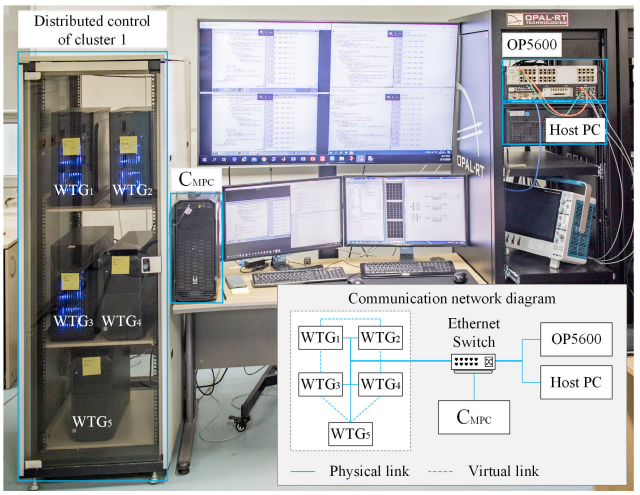

FIGURE 11. Real-time simulation platform.

consists of a real-time simulator OP5600, a host computer that utilizes the RT-LAB to model the offshore wind farm system and generates the executable codes for real-time simulator, a central control computer that is used to implement the centralized predictive voltage controller (C_{MPC}), and five computers that implement the distributed control layer of cluster 1. Modbus Ethernet TCP/IP is used to communicate these devices and the communication network diagram is also shown in Fig. 10. The OP5600 simulator sends the information of total reactive powers of all clusters (Q_{ci}) and the PCC voltage (v_{pcc}) to the central controller. The optimal control actions (u_{MPC}) that minimize the PCC voltage variation are calculated then they are sent to the simulator OP5600. The consensus-based distributed cluster control layers of cluster 2 and 3 are implemented in the OP5600 simulator.

It is assumed that the PCC voltage drops 10% at 20 s and the wind farm controller regulates the total output reactive power to recover the PCC voltage. The proposed control strategy is compared with the full consensus control that only utilizes the distributed control layer and the local control layer to regulate the PCC voltage. Since the performance of the

full consensus control strategy depends significantly on the communication network topology, two connection types of communication networks are investigated, which are the ring and cross connections, as shown in Fig. 12.

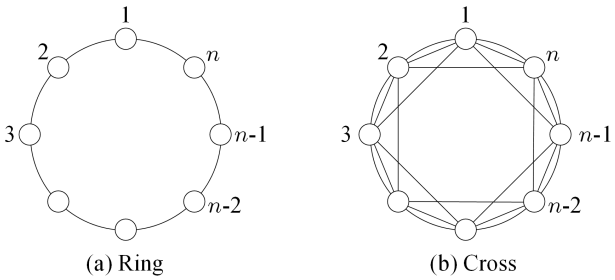

FIGURE 12. Two topologies of communication network in the full consensus control strategy ($n = 30$).

A. PCC VOLTAGE CONTROL PERFORMANCE

The output reactive powers of WTGs under the proposed predictive control strategy is shown in Fig. 13. It can be seen that the output reactive powers of all WTGs are proportional to their capability. The power rating of WTG in cluster 3 is the smallest, resulting in the smallest reactive power supply compared to other clusters. By comparison, the reactive power output of WTGs in cluster 1 is the largest. It can be observed that the WTGs in each cluster equally share their reactive power generation. The convergence time of output reactive powers in each cluster is about 15 s. The control performance of the full consensus control algorithm with ring and cross-communication topologies are shown in Figs. 14 and 15. In the case of using the ring connection, the output reactive power in cluster 1 reaches their limits of 10 MVAr due to slow convergence time. For the cases of clusters 2 and 3, the convergence time is significant (larger than 300 s) due to the large number of WTGs. The convergence time is improved by increasing the communication link like the cross topology, as shown in Fig. 15. The convergence time is significantly reduced from 300 s to 40 s by applying the cross-connection.

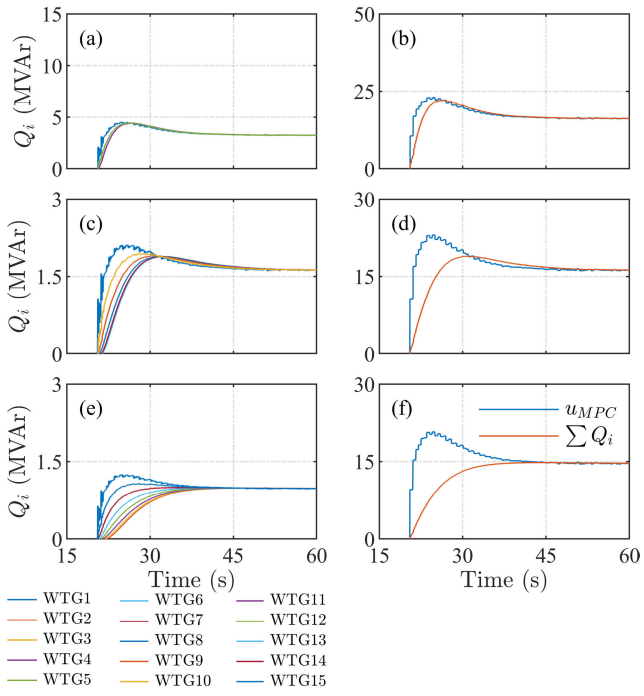

FIGURE 13. Output reactive powers and control commands from central control under proposed strategy: (a), (c), and (d) show the output reactive powers of WTGs in three clusters; (b), (d), and (e) show the control commands for three clusters from the centralized predictive voltage control.

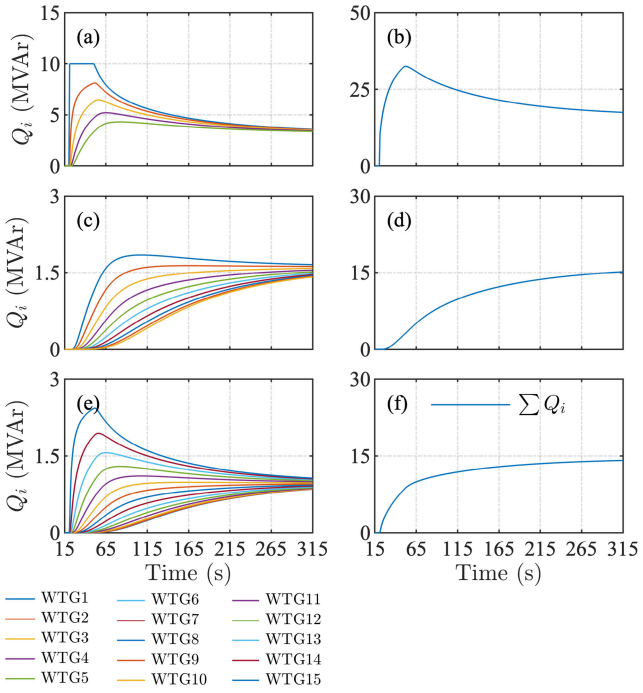

FIGURE 14. Output reactive powers of WTGs under the consensus control with the communication topology of ring type: (a), (c), and (d) show the output reactive powers of WTGs in three clusters; (b), (d), and (e) show the total reactive powers of three clusters.

The total output reactive power of the offshore wind farm system and the waveform of PCC voltage (v_{pcc}) under grid voltage disturbance is shown in Fig. 16. It can be observed that the proposed control strategy shows superior performance compared to the full distributed control schemes. The response of PCC voltage is much quicker due to the fast convergence time of each cluster. The consensus control with the ring communication topology shows the slowest voltage response since the convergence time is significant.

B. MODEL ERROR

It is anticipated that the performance of the predictive voltage control strategy relies on the accuracy of the system model. Thus, this section investigates the performance of the proposed strategy in case the errors exist in the estimation of

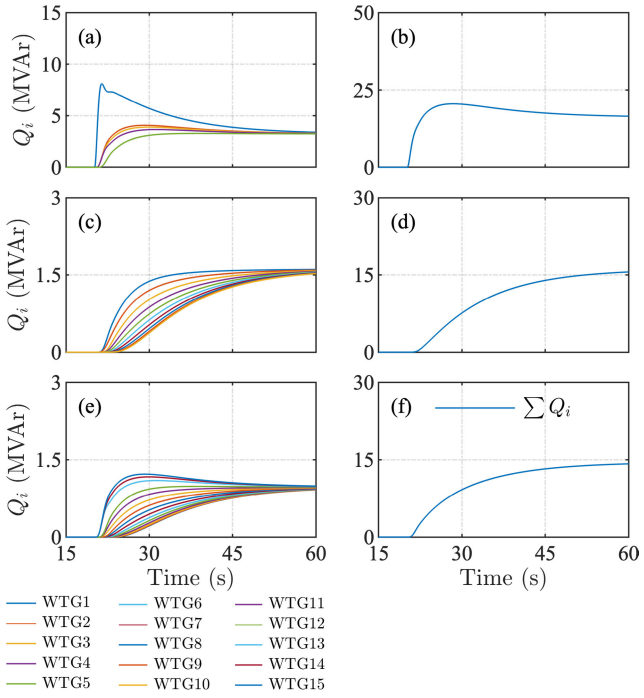

FIGURE 15. Output reactive powers of WTGs under the consensus control with the communication topology of cross type: (a), (c), and (d) show the output reactive powers of WTGs in three clusters; (b), (d), and (e) show the total reactive powers of three clusters.

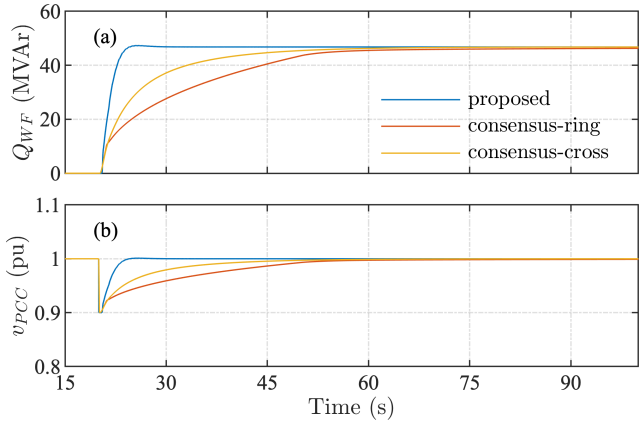

FIGURE 16. Comparison of three control strategies: (a) total reactive power of offshore wind farm required to compensate for the voltage disturbance; (b) PCC voltage responses.

cluster models, which are caused by the existence of cable impedance, the communication delay or failure of communication links. These errors have impacts on the convergence time (τ_i), which directly affect to the estimation of time constant (τ_{ci}). The control performance of the proposed strategy is investigated in the conditions of significant error of time constant τ_{ci}, which is between -50% to $+50\%$. The eigenvalues of the predictive voltage control of the offshore wind farm system under the system error, which is calculated by (41), is shown in Fig. 17. It can be seen that the wind farm control system is stable since all eigenvalues are located inside the unit circle. The time-domain responses of output reactive

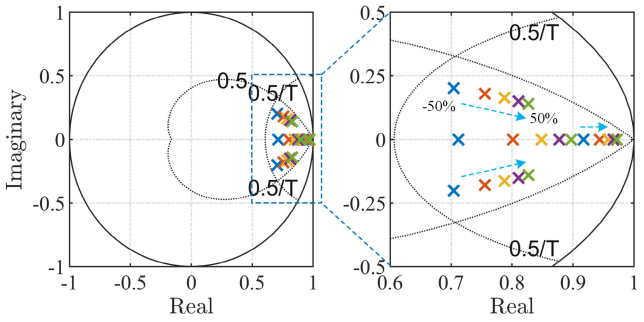

FIGURE 17. Eigenvalues of the predictive voltage control in case error occurs in the estimation of the cluster models.

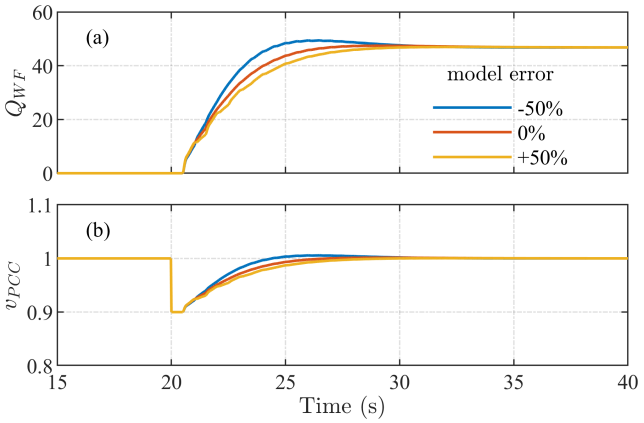

FIGURE 18. Responses of wind farm reactive power and PCC voltage in case of model error.

power and PCC voltage are shown in Fig. 18, which shows a slight impact by the significant error of the model estimation.

C. LARGE-SCALE WIND FARM CONTROL

The proposed wind farm control strategy is verified in the large-scale wind farm systems, in which the number of WTGs is 600 and they are divided into 60 clusters. The maximum number of WTGs in one cluster is 15 to guarantee the fast convergence speed of the distributed cluster control. Fig. 19 shows the responses of output reactive power and

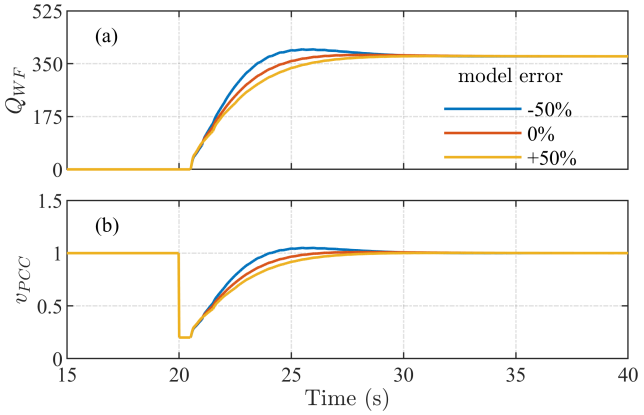

FIGURE 19. Output reactive power of offshore wind farm and PCC voltage response in case of large-scale wind farm system with 600 WTGs: (a) total output reactive power; (b) PCC voltage response.

PCC voltage. Although the offshore wind farm consists of a significant number of WTGs, the proposed control strategy quickly recovers PCC voltage after disturbance (about 5 s), as shown in Fig. 19(b). The eigenvalues of the wind farm control system under model error are shown in Fig. 20, which indicates the stable control of the proposed strategy.

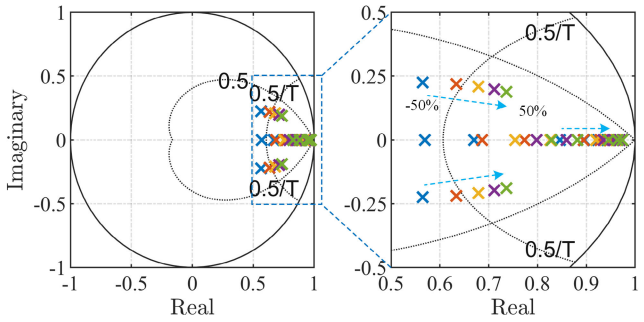

FIGURE 20. Eigenvalues of the 600-WTG wind farm system in case the estimation error varies from −50% to +50%.

The computation time of the predictive controller is an important factor for the design of the practical control system. Fig. 21 shows the computation time of the predictive voltage controller with respect to the number of variables. It could be seen that the computation time significantly increases when the number of variables is larger than 300. In the case the wind farm system consisting of 600 WTGs, the computation time of the conventional centralized predictive voltage controller reaches 0.8 s whereas it is less than 0.1 s in the case of the proposed wind farm controller (wind farm with 60 clusters). It should be noted that the computation time of the predictive controller should be smaller than the sampling time (T_{MPC}) to ensure a stable control system. The increase in the computation time results in the increase of sampling time, leading to the slow response of the central control system. The proposed hybrid control method could significantly reduce the number of variables and the computation time.

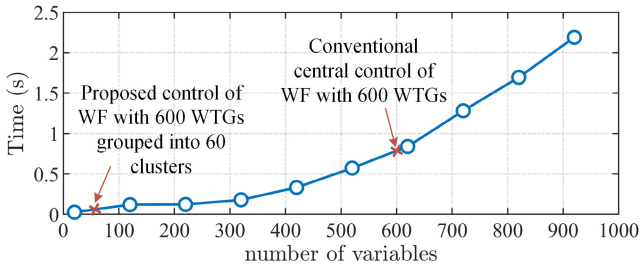

FIGURE 21. Computation time of the model predictive controller versus the number of variables, in which the variables could be the clusters in the proposed predictive control or the WTGs in the conventional central control method.

IV. CONCLUSION

The hybrid control method based on the distributed cluster control and the centralized predictive voltage control offers both advantages of the central and decentralized control methods such as fast control response and high reliability. The comparison studies on the proposed method and the full distributed wind farm control based on the consensus algorithm showed the superior performance of the proposed controller in terms of reactive powers and PCC voltage responses. Accurate reactive power sharing among WTGs could be easily maintained by involving additional constraints in the proposed method. Eigenvalue analysis has shown the stability and robustness of the proposed predictive voltage control method in the condition of significant model errors. Based on the computation time analysis of the proposed predictive controller, a proper number of clusters could be chosen for practical applicability. In addition, the control-hardware-in-the-loop simulation verified the feasibility of the proposed controller for the practical application. The proposed method would be a promising solution for the large-scale offshore wind farm control since it overcomes the problems in both central and decentralized control methods.

It should be noted that the grid voltage v_{grid} can change significantly in case of weak grid, the development of the state-space model for the design of central MPC strategy should consider the effect of grid voltage variation. The proposed controller in this study is considered for the strong grid system to show the feasibility and effectiveness of the proposed hybrid control strategy based on distributed and centralized controllers. The proposed controller in this study could be further improved to apply for the weak grid system.

REFERENCES

[1] Y.-K. Wu, P.-E. Su, Y.-S. Su, T.-Y. Wu, and W.-S. Tan, "Economics- and reliability-based design for an offshore wind farm," *IEEE Trans. Ind. Appl.*, vol. 53, no. 6, pp. 5139–5149, Dec. 2017.

[2] J.-A. Perez-Rua and N. A. Cutululis, "Electrical cable optimization in offshore wind farms—A review," *IEEE Access*, vol. 7, pp. 85796–85811, 2019.

[3] M. J. Hossain, H. R. Pota, M. A. Mahmud, and R. A. Ramos, "Investigation of the impacts of large-scale wind power penetration on the angle and voltage stability of power systems," *IEEE Syst. J.*, vol. 6, no. 1, pp. 76–84, Mar. 2012.

[4] N. R. Ullah, K. Bhattacharya, and T. Thiringer, "Wind farms as reactive power ancillary service providers—Technical and economic issues," *IEEE Trans. Energy Convers.*, vol. 24, no. 3, pp. 661–672, Sep. 2009.

[5] G. Tapia, A. Tapia, and J. X. Ostolaza, "Proportional–integral regulator-based approach to wind farm reactive power management for secondary voltage control," *IEEE Trans. Energy Convers.*, vol. 22, no. 2, pp. 488–498, Jun. 2007.

[6] R. Blasco-Gimenez, S. Añó-Villalba, J. Rodríguez-D'Derlée, F. Morant, and S. Bernal-Perez, "Distributed voltage and frequency control of offshore wind farms connected with a diode-based HVdc link," *IEEE Trans. Power Electron.*, vol. 25, no. 12, pp. 3095–3105, Dec. 2010.

[7] M. A. Cardiel-Alvarez, S. Arnaltes, J. L. Rodriguez-Amenedo, and A. Nami, "Decentralized control of offshore wind farms connected to diode-based HVdc links," *IEEE Trans. Energy Convers.*, vol. 33, no. 3, pp. 1233–1241, Sep. 2018.

[8] M. El Moursi, G. Joos, and C. Abbey, "A secondary voltage control strategy for transmission level interconnection of wind generation," *IEEE Trans. Power Electron.*, vol. 23, no. 3, pp. 1178–1190, May 2008.

[9] H. Zhao, Q. Wu, Q. Guo, H. Sun, S. Huang, and Y. Xue, "Coordinated voltage control of a wind farm based on model predictive control," *IEEE Trans. Sustain. Energy*, vol. 7, no. 4, pp. 1440–1451, Oct. 2016.

[10] Y. Guo, H. Gao, Q. Wu, H. Zhao, J. Ostergaard, and M. Shahidehpour, "Enhanced voltage control of VSC-HVDC-Connected offshore wind farms based on model predictive control," *IEEE Trans. Sustain. Energy*, vol. 9, no. 1, pp. 474–487, Jan. 2018.

[11] H. Zhao, Q. Wu, J. Wang, Z. Liu, M. Shahidehpour, and Y. Xue, "Combined active and reactive power control of wind farms based on model predictive control," *IEEE Trans. Energy Convers.*, vol. 32, no. 3, pp. 1177–1187, Sep. 2017. [Online]. Available: https://ieeexplore.ieee.org/document/7820089
[12] Y. Guo, H. Gao, H. Xing, Q. Wu, and Z. Lin, "Decentralized coordinated voltage control for VSC-HVDC connected wind farms based on ADMM," *IEEE Trans. Sustain. Energy*, vol. 10, no. 2, pp. 800–810, Apr. 2019.
[13] S. Asadollah, R. Zhu, and M. Liserre, "Analysis of voltage control strategies for wind farms," *IEEE Trans. Sustain. Energy*, vol. 11, no. 2, pp. 1002–1012, Apr. 2020.
[14] S. Huang, Q. Wu, J. Zhao, and W. Liao, "Distributed optimal voltage control for VSC-HVDC connected large-scale wind farm cluster based on analytical target cascading method," *IEEE Trans. Sustain. Energy*, vol. 11, no. 4, pp. 2152–2161, Oct. 2020.
[15] X. Liu, Y. Zhang, and K. Y. Lee, "Coordinated distributed MPC for load frequency control of power system with wind farms," *IEEE Trans. Ind. Electron.*, vol. 64, no. 6, pp. 5140–5150, Jun. 2017.
[16] H. Zhao, Q. Wu, Q. Guo, H. Sun, and Y. Xue, "Distributed model predictive control of a wind farm for optimal active power controlpart II: Implementation with clustering-based piece-wise affine wind turbine model," *IEEE Trans. Sustain. Energy*, vol. 6, no. 3, pp. 840–849, Jul. 2015.
[17] H. Zhang, S. Kim, Q. Sun, and J. Zhou, "Distributed adaptive virtual impedance control for accurate reactive power sharing based on consensus control in microgrids," *IEEE Trans. Smart Grid*, vol. 8, no. 4, pp. 1749–1761, Jul. 2017.
[18] I. Khan, Y. Xu, H. Sun, and V. Bhattacharjee, "Distributed optimal reactive power control of power systems," *IEEE Access*, vol. 6, pp. 7100–7111, 2018.
[19] X. Wu, Y. Xu, J. He, X. Wang, J. C. Vasquez, and J. M. Guerrero, "Pinning-based hierarchical and distributed cooperative control for AC microgrid clusters," *IEEE Trans. Power Electron.*, vol. 35, no. 9, pp. 9867–9887, Feb. 2020.
[20] Y. Fan, G. Hu, and M. Egerstedt, "Distributed reactive power sharing control for microgrids with event-triggered communication," *IEEE Trans. Control Syst. Technol.*, vol. 25, no. 1, pp. 118–128, Jan. 2017.
[21] J. Schiffer, T. Seel, J. Raisch, and T. Sezi, "Voltage stability and reactive power sharing in inverter-based microgrids with consensus-based distributed voltage control," *IEEE Trans. Control Syst. Technol.*, vol. 24, no. 1, pp. 96–109, Jan. 2016.
[22] R. Han, L. Meng, G. Ferrari-Trecate, E. A. A. Coelho, J. C. Vasquez, and J. M. Guerrero, "Containment and consensus-based distributed coordination control to achieve bounded voltage and precise reactive power sharing in islanded AC microgrids," *IEEE Trans. Ind. Appl.*, vol. 53, no. 6, pp. 5187–5199, Nov. 2017.
[23] J. Lai, X. Lu, X. Li, and R.-L. Tang, "Distributed multiagent-oriented average control for voltage restoration and reactive power sharing of autonomous microgrids," *IEEE Access*, vol. 6, pp. 25551–25561, 2018.
[24] C. Dou, Z. Zhang, D. Yue, and Y. Zheng, "MAS-based hierarchical distributed coordinate control strategy of virtual power source voltage in low-voltage microgrid," *IEEE Access*, vol. 5, pp. 11381–11390, 2017.
[25] X. Fan, E. Crisostomi, D. Thomopulos, Z. Baohui, R. Shorten, and S. Yang, "An optimized decentralized power sharing strategy for wind farm de-loading," *IEEE Trans. Power Syst.*, early access, Jul. 9, 2020, doi: 10.1109/TPWRS.2020.3008258.
[26] Y. Guo, H. Gao, D. Wang, and Q. Wu, "Online optimal feedback voltage control of wind farms: Decentralized and asynchronous implementations," *IEEE Trans. Sustain. Energy*, early access, Jun. 12, 2020, doi: 10.1109/TSTE.2020.3002094.

THAI-THANH NGUYEN (Member, IEEE) received the B.S. degree in electrical engineering from the Hanoi University of Science and Technology, Vietnam, in 2013, and the Ph.D. degree in electrical engineering from Incheon National University, South Korea, in 2019. From 2019 to 2020, he was a Postdoctoral Research Associate with Incheon National University. Since November 2020, he has been a Research Associate with Clarkson University, Potsdam, NY, USA. His research interests include power system control and stability, power converter control, and application of power electronics to power systems.

HAK-MAN KIM (Senior Member, IEEE) received the Ph.D. degree in electrical engineering from Sungkyunkwan University, South Korea, in 1998, and the Ph.D. degree in information sciences from Tohoku University, Japan, in 2011. From October 1996 to February 2008, he worked with the Korea Electrotechnology Research Institute (KERI), South Korea. He is currently a Professor with the Department of Electrical Engineering, Incheon National University, South Korea. His research interests include microgrid operation and control, and dc power systems.